Unrequited Love: Estimating the Electoral Effect of a Place-based Green Subsidy with a 2D Regression Discontinuity Design

Zikai Li*

October 13, 2025

Abstract

Can green tax credits targeted at areas vulnerable to economic decline shift voter support? Advocates argue that economic gains from such incentives can realign political preferences by altering local communities' cost-benefit calculations. However, competing mechanisms such as disruptions to these communities and ideological resistance may offset these effects or even trigger backlash. Focusing on the Energy Community Tax Credit Bonus (ECTCB) under the 2022 Inflation Reduction Act, I use a two-dimensional regression discontinuity (2DRD) design to estimate its impact on the Democratic share of the two-party vote in the 2024 presidential election. The analysis provides causal evidence that the policy failed to achieve its intended political objective: rather than increasing support for the incumbent party, the results indicate a small negative effect (point estimate: -0.0039; 95% confidence interval: $[-0.0078, -0.0002]$). This paper also makes methodological contributions by developing and validating an improved 2DRD estimator that integrates bagging with bootstrap-based inference.

Keywords: greenlash, green policy, place-based policy, climate policy, Inflation Reduction Act, industrial policy, multidimensional regression discontinuity design

*PhD Candidate, Department of Political Science, University of Chicago. I'm grateful to Parrish Bergquist, Andrew Eggers, Anthony Fowler, Robert Gulotty, Molly Offer-Westort and Anton Strezhnev for their feedback. I thank Zhijie Huang for research assistance and the Social Sciences Computing Services at the University of Chicago for computational support. For helpful comments, I thank workshop participants at the University of Chicago. For financial support, I thank the National Science Foundation and the American Political Science Association. All errors are my own.

1 Introduction

The Texarkana metropolitan statistical area (MSA) straddles Bowie County in Texas and Miller County in Arkansas. In 2022, this small Southern community's unemployment rate of 4.3% exceeded the national average by 0.7 percentage points, while its fossil fuel employment had declined from a peak of 0.9% in 2011. Because of its history of fossil fuel employment and elevated unemployment, the Inflation Reduction Act (IRA) designated Texarkana as an Energy Community, a designation that made the area eligible for enhanced tax credits for renewable energy projects, the Energy Community Tax Credit Bonus (ECTCB). Renewable energy projects in the area have seen a significant boom. For example, in March 2023, the TexAmericas Center, owner and operator of a 12,000-acre Texarkana industrial park, announced plans to dedicate 400 acres for the development of "green energy data centers, suitable for major companies looking to expand and enhance data storage capabilities." Yet this transformation takes place within a political context that would suggest skepticism toward renewable energy: the MSA gave just 27.5% of its two-party vote to the Democratic candidate in the 2020 presidential election. How did the ECTCB change this in 2024, if at all? While the policy could potentially have benefited the incumbent party, multiple competing mechanisms made the electoral impact of these clean energy incentives difficult to predict in advance.

In this paper, I examine how place-based incentives for green investments affect political behavior in regions vulnerable to economic decline. Among scholars and practitioners, interest in the political consequences of place-based climate policies has increased, though consensus remains limited. Supporters see targeted economic development as a key tool to arrest the rise of populism (The Economist 2016).[1] They consider place-based policies to be instruments for driving local economic change and political shifts. Applied to climate policies, this perspective suggests that delivering economic benefits may alter the cost-benefit

[1] In comments after the 2024 US elections, some observers noted that industrial policies aimed at winning over working-class voters had been "hardly a far-fetched or unserious theory" ex ante (Rosenfeld & Schlozman 2025, Rodrik 2024).

calculations of local stakeholders, potentially encouraging them to support further climate measures. This "catalyst" view suggests that reducing barriers to renewable projects will nudge communities to be more open toward the green transition.

These place-based tools occur in the context of broader state-led efforts to decarbonize the economy. Such policies redirect economic activity away from fossil fuel industries, creating both opportunities and disruptions. Regions dependent on coal, oil, or natural gas production often resist these changes. Communities expecting job losses (Pollin & Callaci 2019) or disruption to cultural identities tied to fossil energy (Carley et al. 2018) frequently oppose renewable energy initiatives and climate policies (Scheiber 2021). From a justice perspective, placing disproportionate transition costs on these communities raises ethical concerns (Carley & Konisky 2020). Electorally, they often have enough political power to stall or limit ambitious climate initiatives (Mildenberger 2020, Scheiber 2021).

Policymakers and researchers have thus advocated for place-based economic approaches to drive clean energy development in regions facing industrial decline. These strategies typically deploy tax incentives, grants, and public investments to stimulate local economies and ease transition concerns (e.g., Bolet et al. 2024, Carley et al. 2018). Such programs serve dual purposes: promoting "just transitions" for affected communities while potentially building political support for broader decarbonization goals (Bergquist et al. 2020). However, establishing causal evidence for their political effectiveness is methodologically challenging. The existing literature relies heavily on survey experiments with hypothetical scenarios or observational designs with strong assumptions for causal identification. Survey experimental research (e.g., Bergquist et al. 2020, Gaikwad et al. 2022) often asks about hypothetical policies and may over- or under-estimate public support compared to real-world implementation (Anderson et al. 2023, Gustafson et al. 2019), as stated preferences often diverge from actual behavior when stakes are concrete rather than abstract.

Observational studies, on the other hand, face challenges with causal identification. Places experiencing industrial decline, particularly those with higher concentrations of fos-

sil fuel employment, differ systematically from other regions in possibly unobservable ways that correlate with political outcomes. These differences may stem from long-standing economic trajectories, cultural characteristics, or other factors. When researchers rely on comparing places with different concentrations of declining industries to draw inferences about the effects of place-based policies or market-driven industrial change, they face challenges distinguishing genuine effects from underlying but unobserved differences between places. For instance, while Bolet et al. (2024) found increased support for Spain's governing party in coal-mining regions after it implemented a major transition assistance program, the gap in electoral support between treated and control municipalities had already widened before the implementation of the policy, raising questions about whether the policy caused the observed change in electoral support. In another study focusing on what appeared to be a place-based shock, Gazmararian (2025) found that the shale boom in the US in 2008 increased Republican vote shares in coal-dependent counties and attributed this to heightened salience of environmental regulations. However, Li & Strezhnev (2025) showed that coal counties were already trending Republican before the shock, suggesting the observed correlation reflected underlying trends of political realignment rather than a causal response to industrial change.

This study examines the Energy Community Tax Credit Bonus (ECTCB) established under the 2022 Inflation Reduction Act. The ECTCB offers an opportunity for more credible causal inference because it uses clearly defined eligibility thresholds based on fossil fuel employment and unemployment rates. Using a two-dimensional regression discontinuity design that exploits these discontinuities in program eligibility, I estimate the causal effect of these enhanced clean energy tax incentives on the Democratic vote share of the two-party vote in the 2024 presidential election.

The results suggest that the ECTCB did not increase electoral support for the incumbent party as many proponents anticipated. Instead, the results indicate a slight negative effect on Democratic vote share (point estimate: -0.0039; 95% bootstrap confidence

interval: $(-0.0078, -0.0002)$). Through Monte Carlo simulations, I demonstrate that my estimation approach exhibits minimal bias and offers greater efficiency than other common methods while still maintaining conservative coverage for confidence intervals.

This paper makes four contributions. First, the findings add to the literature on the consequences of green industrial policies by offering new causal estimates of a prominent place-based subsidy's electoral impact. The results help adjudicate between competing expectations about the political effects of green investments in communities vulnerable to economic decline and suggest that the economic benefits of such policies may not be sufficient to overcome other effects on the communities that can dampen support.

Second, while existing work on place-based policies tends to focus on economic outcomes (Busso et al. 2013) or direct government assistance (Bolet et al. 2024, Heddesheimer et al. 2024), this study broadens the scope by examining the political effects of a place-based tax credit bonus for green investments.

Third, this study offers causal evidence on the electoral effect of a climate policy in the United States, the world's second-largest carbon emitter by economic production and the largest by consumption. The political debate over the clean energy transition remains heated and climate policy-making at the federal level is fraught with uncertainty from one administration to the next. Regions experiencing industrial decline are politically powerful, perhaps more so than in many other developed countries, due in part to U.S. electoral institutions. These communities' response to climate policies targeting them is thus particularly consequential for the broader transition both in the U.S. and globally.

Fourth, this paper advances methodological approaches in evaluating the effects of policies and programs with more than one eligibility threshold and a limited effective sample size. I refine a nonparametric method for two-dimensional regression discontinuity designs (Cheng 2023) by integrating insights from the statistics literature on bootstrapping and model selection. Through a simulation study, I show that the new estimator is less

biased and more efficient than existing approaches.[2]

The remainder of the paper is structured as follows. I first provide some background on place-based climate policies and their potential political effects. I then describe the ECTCB and the EC designation process. Next, I present the empirical strategy and a simulation study that evaluates the performance of the point and uncertainty estimators for my estimand. I then present the main results and conclude with a speculative discussion of their implications.

2 Do Place-based Green Policies Affect Political Behavior?

Policy-makers that champion place-based climate policies aim to build political support for decarbonization by targeting regions at risk of economic decline. Such measures channel resources——often in the form of tax incentives and direct grants——directly into communities that might be left behind economically. By mitigating economic threats, advocates hope these policies will dampen local resistance to climate reforms. Yet whether these interventions reliably yield electoral dividends remains an open question.

Place-based policies target assistance geographically. Over the years, governments have adopted such measures outside the climate sphere——for instance, Empowerment Zones (Busso et al. 2013) or Opportunity Zones in the United States——to stimulate investment in poorer areas. Discretionary decisions often shape which areas qualify for assistance, allowing partisan or political motives to creep into the designation process (Frank et al. 2022). This can complicate causal inference about the political and economic effects of such policies.

Place-based measures can influence politics through policy feedback mechanisms. Government policies often do more than create material changes; they reshape how citizens per-

[2]More generally, Cattaneo et al. (2025) show that using univariate distance–to–boundary methods for a multidimensional regression discontinuity design can lead to irreducible misspecification bias whenever the assignment boundary is kinked or irregular.

ceive government legitimacy and their economic interests (Pierson 1993, Campbell 2003). By strategically allocating resources, place-based interventions potentially alter political coalitions. Some scholars emphasize that visible benefits generate gratitude among recipients, who reward politicians responsible for these policies (Soss & Schram 2007, Lerman & McCabe 2017, Simonovits et al. 2021). This suggests targeted climate investments could build electoral support in regions resistant to green transitions. Yet others warn of potential backlash when policies appear to threaten local values or when benefits remain obscure relative to costs (Patashnik 2023).

These feedback effects operate alongside broader economic mechanisms. Regions experiencing economic disruption often develop political resentments that manifest as opposition to mainstream parties (Autor et al. 2020, Colantone & Stanig 2018, Schöll & Kurer 2024, Cremaschi et al. 2024, Cramer 2016). Climate programs that stabilize such economies might help prevent shifts toward political extremes. In a few cases in Europe, for example, targeted regional aid appears to have reduced Euroscepticism and limited support for anti-establishment parties (Schraff 2019, Gold & Lehr 2024, Vergioglou 2023). But some interventions produce counterintuitive results——as in Germany, where eliminating a manufacturing subsidy strengthened support for the political center (Heddesheimer et al. 2024). Similarly, research on America has yielded inconsistent findings on whether and how federal spending boosts incumbent support (Stein & Bickers 1994, Kriner & Reeves 2012). These contradictory findings highlight why we need more empirical research on the politics place-based policies.

Research on the spatial politics of climate policies has also reached mixed conclusions. Survey evidence suggests that bundling economic support with climate action can create broad-based coalitions (Bergquist et al. 2020, Budolfson et al. 2021). In Spain, the "Just Transition Agreement" in coal-mining regions provided resources to assist laid-off miners and was associated with electoral support for the governing party in the following election (Bolet et al. 2024). In the United States, installing wind turbines correlates with increased

Democratic vote shares, presumably because new jobs or tax revenues sway local attitudes (Urpelainen & Zhang 2022). Yet other cases suggest potential backlash. For example, residents near Canadian wind projects blamed the provincial government for perceived overreach, penalizing it at the polls (Stokes 2016).

2.1 Competing Mechanisms

Several mechanisms help explain these different political responses. First, changes in local material conditions can influence political behavior in both expected and unexpected ways. When government incentives boost job creation and infrastructure, residents might credit policy architects (Kriner & Reeves 2012). However, green energy projects often have diffuse benefits and concentrated costs (Stokes 2016). Even if aggregate benefits outweigh costs, the net political effect could be negative if costs are more salient or if benefits come with adverse side effects like rising prices or increased congestion.

Second, cultural and identity factors hinder their political effectiveness. Policies designed to facilitate green transitions might be seen as intrusions on local autonomy or threats to embedded identities. In regions dominated by fossil fuel industries, working-class voters——especially men——often derive significant psychosocial benefits from traditional industries (Lamont 2002, Edin et al. 2019). Even if they benefit economically from green initiatives, threats to industries central to personal and communal identities may drive discontent (Kojola 2019, Bell & York 2010).

Third, the visibility of policy benefits affects how material changes translate into electoral responses. In many place-based programs, funds flow through tax credits or private partnerships, making government involvement less apparent (Mettler 2010). Because people often attribute new jobs to market dynamics rather than public subsidies, "submerged" policies may fail to garner political credit.

Last but not least, most of the studies on the political effects of place-based climate policies rely on observational data. The assumptions required for causal inference vary in their

plausibility across observational studies, which might also partly explain the mixed results. I contribute to these debates by examining the impact of a prominent place-based green policy on U.S. electoral behavior with a two-dimensional regression discontinuity (2DRD) design. The design exploits the discontinuities in eligibility for the Energy Community Tax Credit Bonus (ECTCB) at the cutoffs and relies on relatively weak assumptions for causal identification.

3 The Energy Community Tax Credit Bonus in the Inflation Reduction Act

In 2023, fossil fuels——petroleum, natural gas, and coal——made up approximately 84% of the total primary energy production in the U.S. (U.S. Energy Information Administration n.d.). In 2021, about 364,000 people are in direct employment related to the extraction, processing, transport, or storage of coal, oil, or natural gas based on the definition that the Department of Treasury (Treasury) uses (Interagency Working Group on Coal and Power Plant Communities and Economic Revitalization n.d.).[3] If indirect employment such as jobs related to the manufacturing and construction of fossil fuel infrastructure is included, one estimate puts the total number of jobs at 1.7 million (Tomer et al. 2021). Fossil fuel production is geographically concentrated and has remained symbolically significant in these regions, particularly in Appalachia, West Virginia, and parts of Pennsylvania, where political support for maintaining the industries persists. If the U.S. were to transition away from carbon-intensive fuels and toward renewable energy sources, the transition would likely have adverse economic effects on communities dependent on fossil fuel production.

In 2022, the Biden administration and Democratic-controlled Congress enacted the Inflation Reduction Act (IRA), which includes provisions to promote renewable energy and

[3]Based on data from the County Business Patterns (CBP) dataset for 2021 from the Bureau of Labor Statistics.

reduce greenhouse gas emissions. Many of these provisions are tax credits for clean energy investment, production and consumption. Along with the tax credits, the IRA introduced the Energy Community Tax Credit Bonus (ECTCB). The ECTCB targets communities adversely affected by the decline of fossil fuel industries as well as general economic distress and provides additional tax incentives for clean electricity investments to be located in these communities. The bonus is available for both the investment tax credit (ITC) and the production tax credit (PTC) for clean energy projects. Both of the tax credits provide the option for direct payments instead of a tax liability reduction (i.e., "direct pay" for non-profit and government entities) and/or allow organizations to monetize the credits by transferring them to an entity with a larger tax liability ("transferability").

3.1 The Energy Community Designation at the Statistical Area Level

The IRA defines ECs for two types of geographical units: statistical areas (SAs)[4] and census tracts. In this analysis, I focus on SAs. The SA-level designation is likely to stimulate short-term economic activity through construction and operation of renewable energy projects and, in the long term, lower electricity costs for residents and businesses in these areas. Utility-scale projects can also generate local tax revenues from electricity sales.

Treasury designates an SA as an EC if it meets both of the following two criteria:

- Fossil Fuel Employment (FFE) Rate: An SA must have 0.17% or greater direct employment related to the extraction, processing, transport, or storage of coal, oil, or natural gas at any time after December 31, 2009.[5]

[4] In this paper, I use the term "statistical area" (SA) to refer to both metropolitan statistical areas (MSAs) and non-MSAs under Treasury's definition. Metropolitan statistical areas (MSAs) are groups of counties or county-equivalents delineated by the Office of Management and Budget (OMB). Treasury thus defines MSAs based on the 2010 Decennial Census (Interagency Working Group on Coal and Power Plant Communities and Economic Revitalization n.d.). Non-MSAs are defined primarily according to the May 2023 Metropolitan and Nonmetropolitan Area Definitions published by the Bureau of Labor Statistics (BLS), which aggregate counties outside MSAs into nonmetropolitan areas. See IRS Notice 2023-29, Appendix A, for a complete list of MSAs and non-MSAs used to determine eligibility for the Energy Community designation.

[5] Instead of meeting this criterion, an SA can also qualify if 25% or greater local tax revenues related to coal, oil, or natural gas industries at any time after December 31, 2009. In practice, Treasury does not use this criterion because information on the industry breakdown of local tax revenues is not widely available.

- Unemployment Rate: An SA must have an unemployment rate at or above the national average unemployment rate for the previous year.

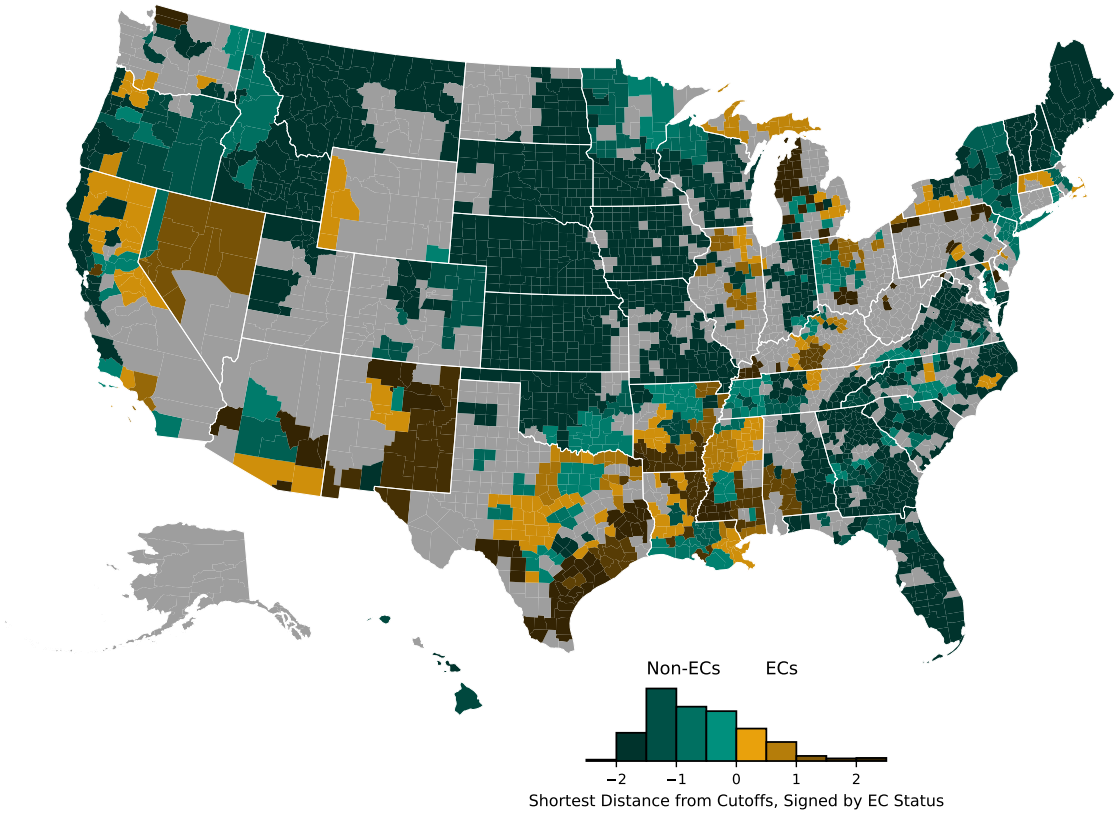

Figure 1: Map of Energy Communities (ECs) and non-ECs at the statistical-area (SA) level in the U.S., shaded by distance to the eligibility boundary. For visualization purposes, I first log-transform and standardize the running variables (after which the two running variables are on the same scale), and then calculate distance as the shortest distance from the eligibility boundary and signed by EC status. Grey areas are not included in the study because they contain census tracts that are "treated" with the EC designation through a different scheme.

Treasury released the first set of EC designations in April 2023. The designations were based on several data sets from the Bureau of Labor Statistics and the Census Bureau. These SAs had had at least 0.17% of direct employment in industries related to the extraction, processing, transportation, or storage of coal, oil, or natural gas for at least one year from 2009 to 2022, and their unemployment rate in 2022 was at or above the national average unemployment rate. Figure 1 shows the distribution of ECs (in yellow) and non-ECs (in

green) in the U.S. The shading indicates the shortest standardized distance to the eligibility boundary, with darker colors indicating greater distance. As the figure shows, the ECs are concentrated in parts of the Appalachian region, the Midwest, the South and the West.

3.2 The Energy Community Tax Credit Bonus (ECTCB)

The ECTCB is increased amounts of the ITC and PTC for projects located in designated Energy Communities (ECs). Table 1 and Table 2 show the investment and production bonus amounts for different project sizes. It is generally a 10% increase in the base credit for the production tax credits and a 1/3 increase in the base credit percentage for the investment tax credits. The bonus is larger in relative terms for energy projects under 1 MW, which are often community solar or wind projects, than for utility-scale projects.[6] The bonus is also larger for projects that meet prevailing wage and apprenticeship requirements, which are designed to ensure that the projects help create high-quality jobs in the communities. Eligible entities cannot receive both the ITC and the PTC for the same facility. In the US, the most prevalent renewable energy sources eligible for the ITC and PTC are solar, wind, and zero- or negative-emission hydropower.

Table 1: Base Investment Credit (48E ITC) and Energy Community Bonus. MW denotes megawatt. *Source*: U.S. Department of Energy (n.d.)

Project Size	Base Credit	Energy Community Bonus
$<$ 1 MW	30%	10%
$>$ 1 MW	6%	2%
$>$ 1 MW and meetsprevailing wage andapprenticeship requirements	30%	10%

[6]To illustrate, a solar farm with a capacity of 1 MW requires between 1 and 10 acres of land depending on the technology and location. It can power about 200 homes in the U.S. for a year, assuming a conversion factor of about 25% and an average annual household electricity consumption of around 10,000 kWh.

Table 2: Base Production Credit (45Y PTC) and Energy Community Bonus. MW denotes megawatt and MWh denotes megawatt hour. *Source*: U.S. Department of Energy (n.d.)

Project Size	Base Credit	Energy Community Bonus
$<$ 1 MW	\$27.50/MWh	\$2.75/MWh
$>$ 1 MW	\$5.50/MWh	\$0.55/MWh
$>$ 1 MW and meetsprevailing wage andapprenticeship requirements	\$27.50/MWh	\$2.75/MWh

4 Inference

I examine the causal impact of the ECTCB at the SA-level on the Democratic two-party vote share in the 2024 presidential election with a two-dimensional regression discontinuity design (RDD). The RDD exploits the discontinuity in the eligibility for the ECTCB at the cutoffs. In this setting, the assignment of treatment (EC status) depends on two separate thresholds, yielding a two-dimensional boundary. To estimate the average treatment effect along this boundary, I adopt a flexible spline-based method (Cheng 2023) to estimate two conditional expectation functions—one for treated units and one for controls—and then integrates their difference over the boundary. This approach preserves information in both dimensions of the running variables, improving efficiency and allowing for treatment effect heterogeneity in either or both dimensions. I first describe the data and the preprocessing steps. Next, I discuss the identifying assumptions, which I argue are highly plausible. I then describe the the estimand, the estimation procedure, and the advantages of the new estimator for the two-dimensional RDD.

4.1 Data

For the variables used to determine eligibility for the ECTCB, I use the data set on 2023 Energy Community designations from Treasury. The data set includes the EC status, the percentages of direct employment in fossil fuel industries from 2010 to 2021, and the 2022 unemployment rate for each statistical area. There are 528 SAs in the data set, of which 142 are designated as ECs.

For the analysis at the SA level, I exclude from the analysis "double-treated" counties (grey areas in Figure 1) with census tracts that are also designated as ECs.[7] I also exclude Alaska because vote counts are not available at a level that can be aggregated to the SA level. Panel A in Figure 2 shows the distribution of the running variables for the remaining 426 SAs, of which 99 are designated as ECs.

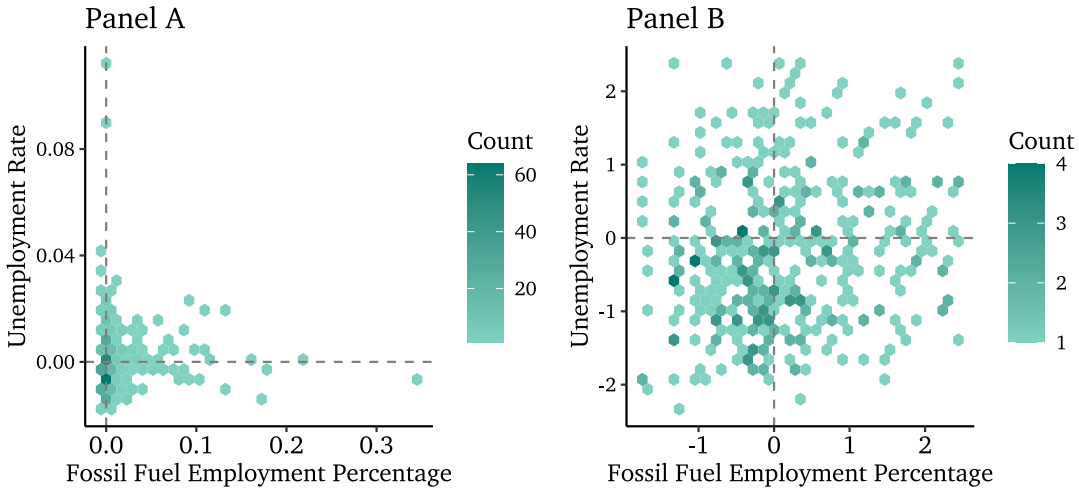

Figure 2: Hexbin plot of the two running variables (unscaled and scaled)

As the figure shows, there are some outlying values for both variables, and the percentage of fossil fuel employment has a long tail. Including the outlying values would not add much to the RD estimation because their density is low and they are far from the eligibility cutoffs. As specified in the pre-analysis plan, I exclude these outlying values from the analysis, log-

[7] Unlike census tracts that are designated as ECs, the SA-level designation does not provide tax credits for manufacturing investments (26 U.S. Code 45C); investment and production tax credits are available only for clean electricity projects in these areas.

transform the percentage of fossil fuel employment, and standardize the variables. See the appendix for the details of this preregistered procedure. Panel B in Figure 2 shows the distribution of the transformed running variables excluding the outliers. In the truncated sample with transformed running variables, the distribution of the running variables is more balanced around the cutoffs. There are 403 SAs in the sample, of which 92 are designated as ECs. This is the working sample I use for the regression discontinuity (RD) analysis.

For presidential vote, I use data from Bloch et al. (2024) for the 2024 election.[8] I aggregate the vote counts for the two major parties from the county level to the SA level. I then calculate the two-party vote share for the Democratic candidate.

4.2 Identifying Assumptions

I use the unemployment and FFE rates at the statistical-area level as running variables to set up the RDD. For causal identification, the key assumption is that the expectations of the potential outcomes are continuous in the running variables at the cutoffs. Pratically, this is likely to hold if (1) lawmakers did not select the thresholds in a way that caused a sharp change in the distribution of SAs at the cutoffs and (2) relevant stakeholders could not precisely manipulate the running variables. These assumptions are highly plausible for the following reaons. First, the Treasury did not finalize the method for calculating FFE rates until eight months after the IRA's passage and later amended it.[^cra_report] Second, FFE rates are derived from the County Business Patterns (CBP) dataset, which includes naturally ocurring and embedded noise. This makes precise manipulation difficult.[9] Third, stakholders cannot easily manipulate the unemployment rate for a given year. Fourth, legislators did not have access to the unemployment rates for 2022 when they passed the IRA

[8] I use the February 18, 2025 version of the data.

[9] Notably, the Census Bureau suppressed certain county-industry employment values in the 2010–2017 CBP data for confidentiality or data quality reasons. For these cells, the data includes only a range of possible values. Treasury assigned a value for each suppressed cell using the midpoint between the lower bound and the average of the lower and upper bounds. By using data with noise to determine eligibility, Treasury introduced additional randomness in EC assignment near the cutoffs. I use the same data to construct the running variables, thus the treatment assignment mechanism aligns with the official procedure.

in August 2022 and did not know which SAs would nearly miss or just meet the national average unemployment rate for 2022.

4.3 Estimand

Let $i = 1, \dots, n$ index the units. Each unit i has a pair of running variables $\mathbf{X}_i = (X_{1,i}, X_{2,i}) \in \mathbb{R}^2$. Define an indicator Z_i for treatment assignment, which is determined by whether $\mathbf{X}_i$ crosses a treatment boundary $\mathcal{B} \subseteq \mathbb{R}^2$:

$$\mathcal{B} = \{(x_1, x_2) \in \mathbb{R}^2 : x_k = 0,\, x_j \geq 0,\, j \neq k,\, k \in \{1, 2\}\}.$$

Each unit i has two potential outcomes, $Y_i(1)$ if treated ($Z_i = 1$) and $Y_i(0)$ if not treated ($Z_i = 0$). The observed outcome for each unit is

$$Y_i = Z_i Y_i(1) + (1 - Z_i) Y_i(0).$$

Following the conventional RD framework, the average treatment effect at a boundary point $\mathbf{x} \in \mathcal{B}$:

$$\begin{aligned}\tau_{\mathbf{x}} =& \mathbb{E}[Y_i(1) - Y_i(0) \mid \mathbf{X}_i = \mathbf{x}] \\ =& \lim_{\epsilon \to 0} \Big(\mathbb{E}\big[Y_i(1) \mid \mathbf{X}_i \in B_\epsilon^1(\mathbf{x})\big] - \mathbb{E}\big[Y_i(0) \mid \mathbf{X}_i \in B_\epsilon^0(\mathbf{x})\big] \Big)\end{aligned}$$

where $B_\epsilon^1(\mathbf{x})$ and $B_\epsilon^0(\mathbf{x})$ denote open balls of radius ϵ centered at $\mathbf{x}$ in the treated and control regions, respectively. The estimand is the average treatment effect along the boundary:

$$\tau = \frac{\int_{\mathcal{B}} \tau_{\mathbf{x}} f_{\mathbf{X}}(\mathbf{x}) d\mathbf{x}}{\int_{\mathcal{B}} f_{\mathbf{X}}(\mathbf{x}) d\mathbf{x}},$$

where $f_{\mathbf{X}}(\mathbf{x})$ is the density of $\mathbf{X}$ at $\mathbf{x}$.

4.4 Estimation Procedure

Estimating a two-dimensional RDD requires modeling how outcomes vary with both $X_{1,i}$ and $X_{2,i}$. One strategy is to reduce the running variables to a univariate measure such as the shortest Euclidean distance to the boundary. However, this strategy can yield misleading confidence intervals when treatment effects vary along either dimension. It also reduces statistical power. Instead, I follow an approach that estimates the difference in conditional expectation functions (CEFs) for treated and control groups directly. Define

$$\mu_1(x_1, x_2) = \mathbb{E}[Y_i(1) \mid X_{1,i} = x_1, X_{2,i} = x_2]$$

and

$$\mu_0(x_1, x_2) = \mathbb{E}[Y_i(0) \mid X_{1,i} = x_1, X_{2,i} = x_2].$$

Following Cheng (2023), I estimate these unknown functions separately by fitting thin plate spline models on the treated and control subsamples. The smoothing parameter is selected by generalized cross-validation, and I apply an undersmoothing adjustment by dividing the penalty parameter by two.

Let and $\hat{\mu}_1(x_1, x_2)$ and $\hat{\mu}_0(x_1, x_2)$ be the undersmoothed versions of the fitted models in the treated and control regions, respectively. Denote the joint probability density function (PDF) of $(X_{1,i}, X_{2,i})$ as $f(x_1, x_2)$, which I estimate using a local likelihood approach. Denote this estimated PDF by $\hat{f}(x_1, x_2)$.

To approximate τ, I form a grid $\mathcal{G}$ along the boundary $\mathcal{B}$ and compute

$$\hat{\tau} = \frac{\sum_{\mathbf{g} \in \mathcal{G}} [\hat{\mu}_1(\mathbf{g}) - \hat{\mu}_0(\mathbf{g})] \hat{f}(\mathbf{g})}{\sum_{\mathbf{g} \in \mathcal{G}} \hat{f}(\mathbf{g})}.$$

For the overall average effect, the grid $\mathcal{G}$ consists of 200 points, with equidistantly spaced 100 points along $X_1 = 0$ and 100 points along $X_2 = 0$ within the observed support. To

estimate the average effect separately for dimension of the boundary, I restrict $\mathcal{G}$ to one axis at a time (e.g., $X_1 = 0$ with X_2 spanning its observed range for the effect along $X_1 = 0$).

4.4.1 Bagging and Confidence Intervals

In a two-dimensional regression discontinuity design, the goal is to identify causal effects along a treatment boundary by modeling how outcomes change near that cutoff. The estimation above relies on flexible, data-driven methods that choose the predictive model based on the observed data. However, such methods can sometimes produce abrupt and erratic changes in the estimated treatment effect at the boundaries between different model regimes (Efron 2014). To mitigate these irregularities, a practical solution is to use bootstrap aggregating, also known as bagging (Breiman 1996). The idea is to repeatedly draw bootstrap samples from the data, run the estimation procedure on each sample, and average the resulting bootstrap estimates to obtain the final point estimate. Bagging achieves algorithmic stability and makes the fitted model less sensitive to specific data points (Soloff et al. 2024). This process smooths out the instability in the nonparametric predictive models for for the CEFs of the potential outcomes, leading to a more stable and reliable estimation of treatment effects along the boundary. Let $\tilde{\mu}_1(x_1, x_2)$ and $\tilde{\mu}_0(x_1, x_2)$ be the average predicted outcomes from the bootstrap samples for (x_1, x_2) under treatment and control, respectively. The bagged estimate of the treatment effect is then

$$\hat{\tau}_{\text{bag}} = \frac{1}{B} \sum_{b=1}^{B} \left[\tilde{\mu}_1(x_1, x_2) - \tilde{\mu}_0(x_1, x_2) \right],$$

where B is the number of bootstrap samples.

To quantify uncertainty, I use a nonparametric delta method (Efron 2014). The intuition behind this approach is that, because the estimate is a smooth function of the data (through the bagging procedure), we can approximate its variability by tracking how changes in the resampled weights affect the treatment effect estimate. In simple terms, across bootstrap

samples, the corresponding changes in the estimated treatment effect reflect the estimator's sensitivity. The estimator aggregates this sensitivity over all observations to provide a robust standard error. In addition to this delta-method standard error, I also compute a percentile bootstrap confidence interval. Section A.2.4 in the Appendix provides technical details on the bagging, the bootstrap method, and the procedure for constructing the delta bootstrap confidence interval. I adjust for pretreatment covariates to increase precision and power. I describe the procedure in Appendix Section A.2.3. In Appendix Section A.3, I also provide a comprehensive simulation study that evaluates the performance of different point and uncertainty estimators, including variants of the bagged estimator described above and an estimator adapted from rdrobust (Calonico et al. 2014), which was designed for one-dimensional RDDs. The simulation study differs from those using synthetic data in that it uses real-world data from the 2020 presidential election in the U.S. as the potential outcome under control to generate the data. The results show that the bagged thin plate spline estimator with delta bootstrap confidence intervals outperforms the other estimators in terms of statistical power (conditional on valid coverage) and root mean squared error (RMSE).

5 Results of the Main Analysis

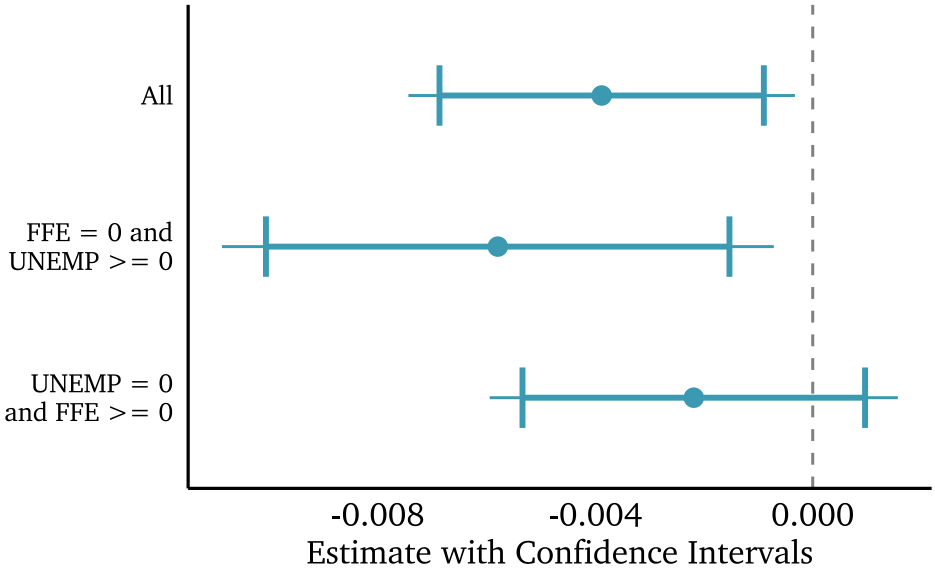

Figure 3: Point estimates for both boundaries combined and each individually with 95% and 90% confidence intervals (CIs). The narrower ranges bounded by bars are 90% CIs and the wider ones are 95% CIs.

Figure 3 visualizes the point estimates for the ATE and the 95% and 90% confidence intervals from the main analysis. The bagging estimate of the ATE is -0.0039. The 95% confidence interval from the nonparametric delta method is $(-0.0074, -0.0003)$ and the p value of 0.032.

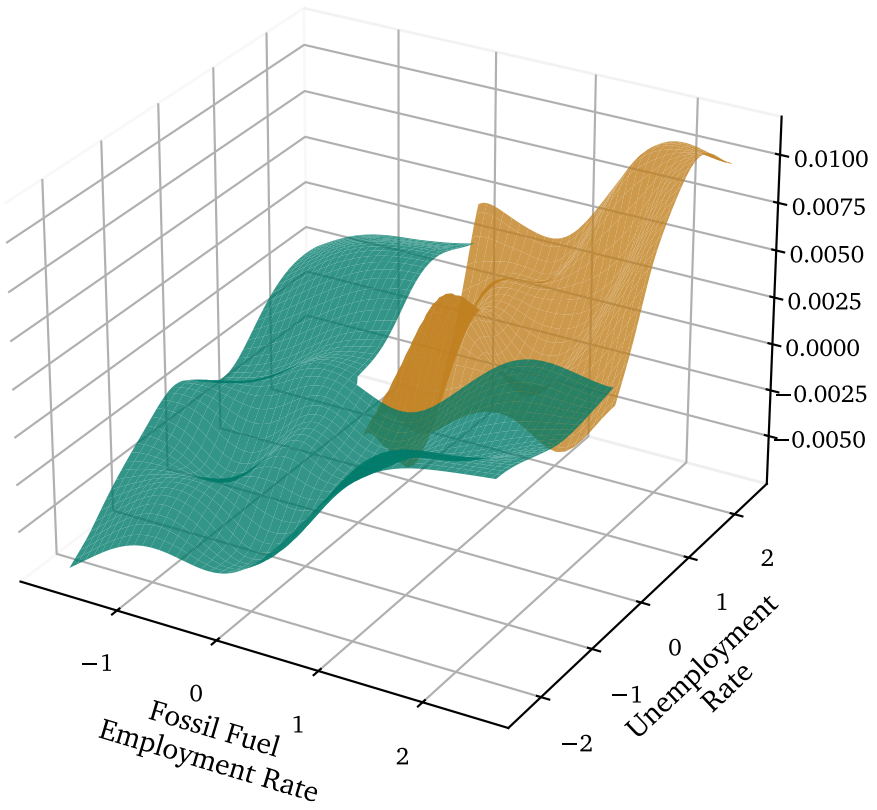

Figure 4: Fitted surfaces for the residualized Democratic vote share in SA-level Energy Communities vs. other SAs in the 2024 presidential election. The larger surface on the left is the untreated region. Predictions are averages of predictions from undersmoothed thin plate spline models across 10,000 bootstrap iterations.

These results show that the ECTCB did not increase the Democratic two-party vote share in the 2024 presidential election and suggests that it reduced the Democratic two-party vote share in the 2024 presidential election by 0.389 percentage points in the SAs near the cutoffs. Figure 4 shows the fitted surfaces for the residualized Democratic vote share in the 2024 presidential election. This is the two-dimensional analog of the one-dimensional RD plot and shows the fitted surfaces for the residualized vote share in Energy Communities (ECs) and non-ECs near the eligibility cutoffs. The figures indicates there is a discontinuity in the residualized vote share at the cutoffs for both running variables. The discontinuity seems to be greater on the treatment boundary where FFE is at its cutoff, i.e., $X_1 = 0, X_2 \geq$

0.

Disaggregating the results by treatment boundaries, I find that point estimate appears to have a larger magnitude on the boundary where $X_1 = 0, X_2 \geq 0$ than on the boundary where $X_1 \geq 0, X_2 = 0$. The point estimate is -0.0058 on the former boundary and -0.0022 on the latter. The negative effect thus appears to be stronger along the cutoff for the FFE rate than for the unemployment rate. The delta-method standard errors are 0.0026 and 0.0020, respectively, which give p-values of 0.0254 and 0.2533. The CIs are $(-0.0124, -0.0001)$ and $(-0.0064, 0.0022)$, respectively. However, the difference in the point estimates is not statistically significant at the 5% level.

Taken together, the results suggest that the Energy Community Tax Credit Bonus (ECTCB) did not boost Democratic votes in 2024 and likely reduced them slightly in ECs near the eligibility cutoffs compared to non-ECs that closely missed the thresholds. This is at odds with claims that place-based green policies can cultivate political goodwill in regions vulnerable to economic disruption.

It is unclear, however, how the estimate generalize well to places far from the cutoffs or to different time frames. The results are derived from areas close to the eligibility thresholds. It is difficult to characterize this subpopulation precisely. From a superpopulation perspective, the population consists of units on the boundary—those with at least one running variable exactly at the cutoff. But because there is no sampling involved, the superpopulation is not well-defined in this context. If we instead consider the cutoffs to be somewhat arbitrary, then the estimate is a weighted average of the treatment effect for all units in the sample, with weights proportional to the ex ante probability that its values of the running variables would be at the cutoffs (Lee & Lemieux 2010). Such weights are probably zero for units far from the cutoffs and higher as units approach the boundary, but the exact shape of the weight function is unknown. Nevertheless, loosely speaking, the units that contribute the most to the estimate in this study are those with unemployment rates close to the national average of 3.65% and/or fossil fuel employment (FFE) shares close to 0.17%.

Because the FFE threshold is fairly low, units that are not very dependent on fossil fuels but have moderate unemployment rates still contribute to the estimate.

Communities with fossil fuel employment shares and/or unemployment rates far from the thresholds may respond differently to the same policy. As with any regression discontinuity design, the estimates speak most directly to the local population near the thresholds in 2024. In addition, the analysis captures effects observed shortly (around 19 months) after policy implementation. The longer-term impact may well diverge in either or both of its direction and magnitude.

6 Discussion

Even though some mechanisms appear to be more plausible than others, the empirical results do not allow for a precise statement about the primary ones driving the observed electoral response. Nevertheless, in this section, I seek to speculate on the mechanisms that may have driven the observed electoral response to the ECTCB.

As discussed in Section 2, several mechanisms could explain a negative electoral response to the ECTCB. One possibility is that renewable energy projects can drive local inflation by increasing land prices when construction activity surges and demand for housing rises, especially if the investors expect the energy projects to have multiplier effects on the local economy in the long run. This inflationary pressure could have dampened voter support for the incumbent party. It is unclear, however, how much of the dislike toward inflation is driven by personal experiences of rising prices versus exposure to media coverage of inflation. If the latter is the primary driver, given the decrease in consumption of local news and the lack of reporting on local inflation, it is unlikely that the inflationary pressure from renewable energy projects would have had a substantial impact on voter behavior. But if the former is the primary driver, the inflationary pressure could have had a more substantial impact. Future research could evaluate the relative plausibility of these two scenarios by

examining if the ECTCB changed how local media outlets covered inflation and how local residents acquired concerns about inflation.

Another mechanism is that renewable energy installations often exacerbate local conflict. A cursory review of news reports and community protests suggest that residents in many communities oppose constructing projects like solar farms and wind turbines close to where they live. This means the perceived cost of renewable energy projects can be highly localized and immediate, while the benefits are long-term and more spatially diffuse. The immediacy and visibility of these conflicts can then contribute to adverse electoral evaluations of the incumbent party.

A third mechanism involves the potential for job displacement and the erosion of cultural identity. Communities with a historical reliance on fossil fuels may experience a sense of loss when traditional industries decline, even if green policies offer alternative economic benefits. In regions like the Texarkana MSA——where fossil fuel employment had been once high but was already very low before the ECTCB—this mechanism might be less pronounced in terms of job displacement, though cultural resistance could still be significant. It is hard to quantify the cultural mechanism without more empirical evidence on how local identity interacts with economic change in these regions.

A more indirect mechanism is the invisibility of the ECTCB. If the ECTCB had been more salient and attributable to the incumbent party, it might have produced a positive effect to help offset the negative effects of the adverse mechanisms discussed above. Future research could investigate how learning about place-based programs like the ECTCB affects voter attitudes.

Several factors could weaken or reverse the overall negative response in other possible worlds. If broader shifts in the national political climate make decarbonization a higher priority, or if communities develop stronger trust in government interventions, such programs could also gain more traction. Further declines in the economic and, by extension, political power of fossil fuel industries—which the ECTCB can help accelerate regardless

of its impact on voter behavior—could also weaken opposition to green policies like the ECTCB.

Alternative program designs could yield different results. The ECTCB is a subsidy that may not have been salient to many residents. More visible or direct benefits, such as job training programs, infrastructure investments, or direct payments to voters laid off by fossil fuel companies, could have different effects on voter behavior. The ECTCB's focus on clean energy projects may also have limited its appeal in regions where fossil fuel industries are deeply embedded in local culture and identity. Programs that support the economic transition to renewable energy while also addressing the noneconomic concerns of affected communities could also be more successful in building political support.

7 References

Anderson, S., Marinescu, I. & Shor, B. (2023), 'Can pigou at the polls stop us melting the poles?', *Journal of the Association of Environmental and Resource Economists* **10**(4), 903–945.

Autor, D., Dorn, D., Hanson, G. & Majlesi, K. (2020), 'Importing political polarization? The electoral consequences of rising trade exposure', *American Economic Review* **110**(10), 3139–3183.

Bell, S. & York, R. (2010), 'Community economic identity: The coal industry and ideology construction in west virginia', *Rural Sociology* **75**(1), 111–143.

Bergquist, P., Mildenberger, M. & Stokes, L. C. (2020), 'Combining climate, economic, and social policy builds public support for climate action in the us', *Environmental Research Letters* **15**(5), 054019.

Bloch, M., Collins, K., Gebeloff, R., Hernandez, M., Khurana, M. & Levitt, Z. (2024), 'Election Results Show a Red Shift Across the U.S. in 2024', *The New York Times* .

URL: *https://www.nytimes.com/interactive/2024/11/06/us/politics/presidential-election-2024-red-shift.html*

Bolet, D., Green, F. & González-Eguino, M. (2024), 'How to get coal country to vote for climate policy: The effect of a "just transition agreement" on spanish election results', *American Political Science Review* p. 1344–59.

Breiman, L. (1996), 'Bagging predictors', *Machine learning* **24**, 123–140.

Budolfson, M., Dennig, F., Errickson, F., Feindt, S., Ferranna, M., Fleurbaey, M., Klenert, D., Kornek, U., Kuruc, K., Méjean, A. et al. (2021), 'Climate action with revenue recycling has benefits for poverty, inequality and well-being', *Nature Climate Change* **11**(12), 1111–1116.

Busso, M., Gregory, J. & Kline, P. (2013), 'Assessing the incidence and efficiency of a prominent place based policy', *American Economic Review* **103**(2), 897–947.

Calonico, S., Cattaneo, M. D. & Titiunik, R. (2014), 'Robust nonparametric confidence intervals for regression-discontinuity designs', *Econometrica* **82**(6), 2295–2326.

Campbell, A. L. (2003), *How Policies Make Citizens: Senior Political Activism and the American Welfare State*, Princeton University Press.

Carley, S., Evans, T. P. & Konisky, D. M. (2018), 'Adaptation, culture, and the energy transition in american coal country', *Energy Research & Social Science* **37**, 133–139.

Carley, S. & Konisky, D. M. (2020), 'The justice and equity implications of the clean energy transition', *Nature Energy* **5**(8), 569–577.

Cattaneo, M. D., Titiunik, R. & Yu, R. R. (2025), 'Estimation and inference in boundary discontinuity designs'.
URL: *https://arxiv.org/abs/2505.05670*

Cheng, A. (2023), 'Estimation of regression discontinuity and kink designs with multiple running variables', *Available at SSRN 4516922* .

Colantone, I. & Stanig, P. (2018), 'The trade origins of economic nationalism: Import competition and voting behavior in western europe', *American Journal of Political Science* **62**(4), 936–953.

Cramer, K. J. (2016), *The Politics of Resentment: Rural Consciousness in Wisconsin and the Rise of Scott Walker*, University of Chicago Press, Chicago.

Cremaschi, S., Rettl, P., Cappelluti, M. & De Vries, C. E. (2024), 'Geographies of discontent: Public service deprivation and the rise of the far right in italy', *American Journal of Political Science* .

Edin, K., Nelson, T., Cherlin, A. & Francis, R. (2019), 'The tenuous attachments of working-class men', *Journal of Economic Perspectives* **33**(2), 211–228.

Efron, B. (2014), 'Estimation and accuracy after model selection', *Journal of the American Statistical Association* **109**(507), 991–1007.

Frank, M. M., Hoopes, J. L. & Lester, R. (2022), 'What determines where opportunity knocks? political affiliation in the selection of opportunity zones', *Journal of Public Economics* **206**, 104588.

Gaikwad, N., Genovese, F. & Tingley, D. (2022), 'Creating climate coalitions: mass preferences for compensating vulnerability in the world's two largest democracies', *American Political Science Review* **116**(4), 1165–1183.

Gazmararian, A. F. (2025), 'Sources of partisan change: Evidence from the shale gas shock in american coal country', *The Journal of Politics* **87**(2), 000–000.

Gold, R. & Lehr, J. (2024), 'Paying off populism: How regional policies affect voting behavior'. Working Paper.

Gustafson, A., Rosenthal, S. A., Ballew, M. T., Goldberg, M. H., Bergquist, P., Kotcher, J. E., Maibach, E. W. & Leiserowitz, A. (2019), 'The development of partisan polarization over the green new deal', *Nature Climate Change* **9**(12), 940–944.

Heddesheimer, V., Hilbig, H. & Wiedemann, A. (2024), 'Place-based policies, local responses, and electoral behavior', *Working Paper* .

Interagency Working Group on Coal and Power Plant Communities and Economic Revitalization (n.d.), 'Energy Community Tax Credit Bonus - FAQs'.
URL: *https://energycommunities.gov/energy-community-tax-credit-bonus-faqs/*

Kojola, E. (2019), 'Bringing back the mines and a way of life: Populism and the politics of extraction', *Annals of the American Association of Geographers* **109**(2), 371–381.

Kriner, D. L. & Reeves, A. (2012), 'The influence of federal spending on presidential elections', *American Political Science Review* **106**(2), 348–366.

Lamont, M. (2002), *The dignity of working men: Morality and the boundaries of race, class, and immigration*, Harvard University Press.

Lee, D. S. & Lemieux, T. (2010), 'Regression discontinuity designs in economics', *Journal of Economic Literature* **48**(2), 281–355.

Lerman, A. E. & McCabe, M. L. (2017), 'Personal experience and public opinion: A theory and test of conditional policy feedback', *Journal of Politics* **79**(2), 624–641.

Li, Z. & Strezhnev, A. (2025), 'Benchmarking parallel trends violations in regression imputation difference-in-differences'.

Mettler, S. (2010), *The Submerged State: How Invisible Government Policies Undermine American Democracy*, University of Chicago Press, Chicago.

Mildenberger, M. (2020), *Carbon captured: How business and labor control climate politics*, MiT Press.

MIT Election Data and Science Lab (2024), 'County Presidential Election Returns 2000-2020'.

Patashnik, E. M. (2023), *Countermobilization: Policy Feedback and Backlash in a Polarized Age*, University of Chicago Press.

Pierson, P. (1993), 'When effect becomes cause: Policy feedback and political change', *World Politics* **45**(4), 595–628.

Pollin, R. & Callaci, B. (2019), 'The economics of just transition: A framework for supporting fossil fuel–dependent workers and communities in the united states', *Labor Studies Journal* **44**(2), 93–138.

Rodrik, D. (2024), 'Why Bidenomics did not deliver at the polls'. Accessed March 06, 2025.
URL: *https://www.project-syndicate.org/commentary/democrats-biden-wrong-kind-of-economic-populism-by-dani-rodrik-2024-12*

Rosenfeld, S. & Schlozman, D. (2025), 'The Democrats' big—-and failed—-bet', *Democracy: A Journal of Ideas* (75).

Scheiber, N. (2021), 'The Achilles' heel of Biden's climate plan? Coal miners'. Accessed October 12, 2024.
URL: *https://nytimes.com/2021/12/08/business/economy/coal-miners-unions-climate.html*

Schraff, D. (2019), 'Regional redistribution and eurosceptic voting', *Journal of European Public Policy* **26**(1), 83–105.

Schöll, N. & Kurer, T. (2024), 'How technological change affects regional voting patterns', *Political Science Research and Methods* **12**(1), 94–111.

Simonovits, G., Malhotra, N., Lee, R. Y. & Healy, A. (2021), 'The effect of distributive poli-

tics on electoral participation: Evidence from 70 million agricultural payments', *Political Behavior* **43**, 737–750.

Soloff, J. A., Barber, R. F. & Willett, R. (2024), 'Bagging provides assumption-free stability', *Journal of Machine Learning Research* **25**(131), 1–35.

Soss, J. & Schram, S. F. (2007), 'A public transformed? Welfare reform as policy feedback', *American Political Science Review* **101**(1), 111–127.

Stein, R. M. & Bickers, K. N. (1994), 'Congressional elections and the pork barrel', *The Journal of Politics* **56**(2), 377–399.

Stokes, L. C. (2016), 'Electoral backlash against climate policy: A natural experiment on retrospective voting and local resistance to public policy', *American Journal of Political Science* **60**(4), 958–974.

Stommes, D., Aronow, P. & Sävje, F. (2023), 'On the reliability of published findings using the regression discontinuity design in political science', *Research & Politics* **10**(2), 20531680231166457.

The Economist (2016), 'Place-based economic policies as a response to populism'.

Tomer, A., Kane, J. W. & George, C. (2021), 'How renewable energy jobs can uplift fossil fuel communities and remake climate politics'.

Urpelainen, J. & Zhang, A. T. (2022), 'Electoral backlash or positive reinforcement? Wind power and congressional elections in the united states', *The Journal of Politics* **84**(3), 1306–1321.

U.S. Department of Energy (n.d.), 'Inflation Reduction Act Tax Credit Opportunities for Hydropower and Marine Energy'.
URL: *https://www.energy.gov/eere/water/inflation-reduction-act-tax-credit-opportunities-hydropower-and-marine-energy*

U.S. Energy Information Administration (n.d.), 'U.S. Energy Facts Explained - Consumption and Production'.
URL: *https://www.eia.gov/energyexplained/us-energy-facts/*

Vergioglou, I. (2023), 'Electoral effects of investment subsidies in national and european elections', *Journal of European Public Policy* **30**(10), 2123–2142.

Weiss, A. (2024), 'How much should we trust modern difference-in-differences estimates?', *Working Paper* .

A Appendix

A.1 Data Preprocessing

I apply the following preregistered adjustments to minimize distortion from extreme values, improve balance near the cutoff and, perhaps most important, bring the two running variables onto a comparable scale.

First, truncation of extremes. I remove observations with running variable values very far from the cutoff. Specifically, any SA with an unemployment-rate running variable more than 0.02 above or below the threshold (i.e. outside the band $-0.02 < X_2 < 0.02$ when centered at the cutoff) is dropped. I also drop SAs with fossil employment shares exceeding 0.15 (15 percentage points above the threshold), which are extreme outliers in X_1. This ensures I focus on areas local to the boundary on both dimensions.

Second, log transformation of FFE. Because raw FFE percentages are highly skewed (many near 0%, a few very high), I transform this variable by taking the log of FFE. In practice, I use $X_1 = \ln(\text{FFE} + 0.0001) - \ln(0.0001)$, which maps an FFE of 0 to 0 and linearizes the lower end of the distribution. This pulls in the right tail and makes the distribution more symmetric.

Third, standardization. I standardize both running variables (FFE and unemployment) by dividing by their respective standard deviations after the above transformations. This puts the two measures on comparable scales so that one does not unduly dominate due to units or magnitude.

A.2 More Details on Estimation Procedure

A.2.1 Advantages of the Two-dimensional RDD over the One-dimensional Design

The two-dimensional RDD has several advantages over one-dimensional designs. First, it allows for treatment effect heterogeneity in either or both of the running variables. In the

empirical setting of this paper, it is plausible that the treatment effect varies with the level of unemployment or FFE. In my simulation study, reducing the dimensionality of the running variables to one can lead to biased estimates and extremely long confidence intervals if the treatment effect is heterogeneous.

Second, it avoids the loss of information that can occur when reducing the dimensionality of the running variables to one. This loss occurs if, for example, the researcher combines the two running variables into one by collapsing them into a single measure of distance to the cutoff. The loss of information can be even greater if the researcher subset the data to those with one running variable above the threshold and use the other running variable as the sole running variable to set up a one-dimensional RDD.

A.2.2 Advantages of Using the Thin Plate Splines

The thin plate spline (TPS) approach offers several advantages over alternative nonparametric methods for our two-dimensional RDD application. First, TPS models performs well at moderate extrapolation beyond the observed data support. TPS maintains reasonable predictive accuracy when extrapolating to points near but outside the observed data range. This property is particularly valuable in RDD applications where we must estimate effects precisely at threshold boundaries where data may be sparse or asymmetrically distributed.

Second, TPS works well with a low-dimensional feature space and a modest sample size. This is a two-dimensional setting with approximately 400 statistical areas. Unlike more data-hungry methods that might require larger samples for stable boundary estimation, TPS can effectively model smooth functions with fewer observations while avoiding overfitting. Its smoothness penalty provides natural regularization that's especially beneficial when estimating boundary effects with limited data.

Having a single penalty parameter also simplifies model selection and tuning (Cheng 2023). Thin plate splines only require choosing a single scalar penalty parameter for an MSE-optimal fit, and need just one estimation procedure to calculate treatment effects

across the boundary. This simplicity allows for straightforward undersmoothing procedures to create valid confidence intervals. In contrast, multidimensional local linear regressions require selecting different bandwidths for each point on the boundary and need separate estimation for each point of interest, making them much more challenging to implement (Cheng 2023).

A.2.3 Covariate Adjustment to Increase Precision and Statistical Power

While modern designs in observational causal inference has increased attention to identification, causally interpretable estimates often suffer from a lack of power (Stommes et al. 2023, Weiss 2024). This is because the "valid" comparisons in credible designs are often far fewer than what the total number of units in the nominal sample would imply, rendering the effective sample size much smaller than the nominal sample size. Fortunately for this study, party vote-shares in US presidential elections are highly predictable with pre-treatment covariates. In US elections, vote share is highly correlated with demographic and socioeconomic characteristics of an area, such as racial composition, share od college graduates, and median income. I can thus increase the power of the study by adjusting for a rich set of covariates in the estimation. I use a two-step procedure recommended by Lee & Lemieux (2010): I first obtain the residuals of the vote share from a prediction model that uses the pre-treatment covariates and then use the residuals as the outcome in the estimation.

The percentage of the population that are white, Black, Hispanic, and Asian, the percentage of the population with a bachelor's degree or higher, the median household income, and the pairwise interactions between these variables can all be predictive of the presidential vote share. Including all of them, however, could lead to overfitting. To avoid this, I implement an elastic net to obtain a predictive model of the outcome at the county level, and use this model to predict the outcome for each SA. To avoid overfitting, I train this model on a semi-independent data source, the counties left out of my main analysis that

belong to treated SAs, and use this model to predict vote shares for the analysis sample. I then aggregate the predicted vote shares to the SA level and residualize the outcome by subtracting the predicted vote share from the observed vote share. I then use the residuals as the outcome in the main analysis.

Below is the list of covariates used in the elastic net model:

- percentage of the total population that is female.
- percentage of the total population that is non-Hispanic White.
- percentage of the total population that is non-Hispanic Black.
- percentage of the total population that is non-Hispanic Asian.
- percentage of the total population that is Hispanic or Latino.
- percentage of the total population with a bachelor's degree or higher.
- percentage of non-Hispanic White individuals with a bachelor's degree or higher.
- percentage of non-Hispanic Black individuals with a bachelor's degree or higher.
- percentage of non-Hispanic Asian individuals with a bachelor's degree or higher.
- percentage of Hispanic or Latino individuals with a bachelor's degree or higher.
- percentage of female non-Hispanic White individuals with a bachelor's degree or higher.
- median household income in 2021.
- Democratic candidate's share of the two-party vote in the 2020 presidential election.
- Democratic candidate's share of the two-party vote in the 2016 presidential election.

In the elastic net model, I also include state dummies. To account for the possibility that the coefficients of the covariates may vary across regions, I interact each covariate from the list above (but not their pairwise interactions) with the following region dummies (note that many of these variables have coefficients that approximately zero after the elastic net regularization):

- Pacific West: Washington, Oregon, California
- Mountain West 1: Montana, Idaho, Wyoming, Utah

- Mountain West 2: Nevada, Colorado, Arizona, New Mexico
- Midwest: Illinois, Indiana, Michigan, Ohio, Wisconsin, Iowa, Kansas, Minnesota, Missouri, Nebraska, North Dakota, South Dakota
- South 1: Texas, Florida, Georgia, North Carolina
- South 2: Alabama, Arkansas, Kentucky, Louisiana, Mississippi, Oklahoma, South Carolina, Tennessee, West Virginia
- Northeast: Connecticut, Maine, Massachusetts, New Hampshire, New Jersey, New York, Pennsylvania, Rhode Island, Vermont, Delaware, Maryland, Virginia, District of Columbia

I use data from the MIT Election Data and Science Lab (2024) for the vote shares in the 2016 and 2020 presidential elections. For general and racial/ethnic population estimates, I use the 7/1/2022 estimates from the Census Bureau's *Annual County Resident Population Estimates by Age, Sex, Race, and Hispanic Origin* (CC-EST2023-ALLDATA). For educational attainment, I use the 2021 5-year estimates from the Census Bureau's *2021: ACS 5-Year Estimates Selected Population Detailed Tables* (ACSDT5YSPT2021.B15002). For median household income in 2021, I use a data set from the US Department of Agriculture's Economic Research Service.[10] For counties missing data on one or more of the covariates above, I impute the values with the median county within each statistical area. By median county, I mean the county with the median percentage of non-Hispanic White individuals. If entire SAs are missing data, I impute the values with the median SA within the state.

A.2.4 Bagging for the Point Estimate and Bootstrap Confidence Intervals

I estimate the models for conditional expectations in the two-dimensional RDD using a flexible, data-driven procedure. This procedure has advantages over traditional parametric methods, which may impose strong assumptions on the functional form of the relationship between the running variables and the outcome. However, such methods can produce un-

[10] https://www.ers.usda.gov/data-products/county-level-data-sets/county-level-data-sets-download-data/

stable estimates if based on a single sample. This is because the estimation happens after data-based model selection,[11] which can produce abrupt changes in values at the boundaries between different model regions (Efron 2014). To reduce this variability, I use bagging, whereby B bootstrap samples are drawn from the original dataset. For each bootstrap sample $i \in \{1, \dots, B\}$, the two-dimensional RDD model is fit to yield a treatment effect estimate τ_i^*. The bagged point estimate is then computed as the average:

$$\bar{\tau} = \frac{1}{B} \sum_{i=1}^{B} \tau_i^*.$$

Because the final estimate $\bar{\tau}$ is an average of many bootstrap estimates, its variability can be approximated by examining how the individual bootstrap weights influence the estimate.[12] Suppose we index the original data by $j \in \{1, \dots, n\}$, and let w_{ij}^* be the weight assigned to observation j in bootstrap sample i. (Each bootstrap sample is drawn such that the weights satisfy $\sum_{j=1}^{n} w_{ij}^* = n$.) Define the average weight for observation j as

$$\bar{w}_j = \frac{1}{B} \sum_{i=1}^{B} w_{ij}^*.$$

For each observation, the sensitivity of the estimate to changes in its weight can be quantified by the covariance between the weight and the bootstrap estimate:

$$\hat{\text{cov}}_j = \frac{1}{B} \sum_{i=1}^{B} \Big(w_{ij}^* - \bar{w}_j \Big) \Big(\tau_i^* - \bar{\tau} \Big).$$

[11] Here, model selection refers to the process of choosing the best-fitting model from a set of candidate models using a data-driven criterion. It does not include the selection of coefficients within a model, such as in an OLS regression with a fixed set of regressors.

[12] I implement the fractional-weights bootstrap, drawing weights for each observation from a Dirichlet distribution. This approach tends to yield a smoother distribution of bootstrapped estimates compared to the standard bootstrap, as it does not entirely exclude any data points in any iteration. This procedure is particularly helpful in my design given the limited number of unique values in the thin-plate spline estimation.

The overall standard error is then approximated by aggregating these contributions:

$$\tilde{\sigma}_B = \sqrt{\sum_{j=1}^{n} \hat{\text{cov}}_j^2}.$$

The intuition is that the sum of the covariances $\hat{\text{cov}}_j$ over all observations reflects the total variability in $\bar{\tau}$ due to fluctuations in the bootstrap weights. This provides an analytically derived standard error without having to rely solely on the empirical distribution of the τ_i^*.

The delta-method confidence interval is:

$$\bar{\tau} \pm z_{0.975}\, \tilde{\sigma}_B$$

where $z_{0.975}$ denotes the 97.5th percentile of the standard normal distribution.

A.2.4.1 Percentile Bootstrap for Robustness

I also construct confidence intervals using the percentile bootstrap method. Let $\{\tau_i^*\}_{i=1}^B$ be the set of bootstrap estimates. The $\alpha/2$ and $1-\alpha/2$ empirical percentiles of these estimates, $q_{\alpha/2}$ and $q_{1-\alpha/2}$, provide an alternative confidence interval:

$$(q_{\alpha/2},\, q_{1-\alpha/2}).$$

Additionally, the two-sided p-value for testing the null hypothesis $\tau = 0$ is computed as:

$$p = 2 \times \min\left\{ \frac{\#\{\tau_i^* \geq 0\}}{B},\, \frac{\#\{\tau_i^* \leq 0\}}{B} \right\}.$$

A.3 Simulation Study Using Data from the 2020 Presidential Election

In each iteration of the simulation, I draw cutoff values from two independent uniform distributions. I choose the range of the uniform distributions to be close to the actual data cutoffs. The treatment status for each unit depends on whether the running variables are

both above the cutoffs: if they are, the unit is treated; otherwise, it is not treated. The observed outcome is the potential outcome under treatment if the unit is treated and the potential outcome under control if the unit is not treated. I then obtain the point estimate and CI using the following methods:

Table 3: The six designs for the simulation study.

Design	Point Estimate	Confidence Interval
1	Thin plate splines (TPS) with bagging	Delta bootstrap (Delta)
2	TPS with bagging	Percentile bootstrap (PCT)
3	TPS without bagging	Bootstrap with normal approximation (Normal)
4	TPS without bagging	Percentile bootstrap (PCT)
5	rdrobust	Robust
6	rdrobust	Bias-corrected (BC)

For designs that use thin plate splines (TPS) to estimate the CEFs, the target estimand is the one defined in the main text:

$$\tau = \frac{\int_{\mathcal{B}} \tau_{\mathbf{x}} f_{\mathbf{X}}(\mathbf{x}) d\mathbf{x}}{\int_{\mathcal{B}} f_{\mathbf{X}}(\mathbf{x}) d\mathbf{x}},$$

where $\tau_{\mathbf{x}}$ is the average treatment effect at a boundary point $\mathbf{x} \in \mathcal{B}$, and $f_{\mathbf{X}}(\mathbf{x})$ is the density of $\mathbf{X}$ at $\mathbf{x}$.

For the rdrobust design, I collapse the two running variables into one by computing each observation's shortest distance from the treatment boundary. First, as in the main analysis, I preprocess the running variables so that they are on the same scale and approximately normally distributed. Then I calculate the distance measure d_i for each observation i as follows:

$$d = \begin{cases} \min\{|X_1|, |X_2|\}, & \text{if } X_1 \geq 0 \text{ and } X_2 \geq 0, \\ X_2, & \text{if } X_1 \geq 0 \text{ and } X_2 < 0, \\ X_1, & \text{if } X_1 < 0 \text{ and } X_2 \geq 0, \\ -\sqrt{X_1^2 + X_2^2}, & \text{if } X_1 < 0 \text{ and } X_2 < 0. \end{cases} \tag{1}$$

Note that, compared to a simple Euclidean distance signed by treatment status, this measure gives rise to an estimand that is comparable to the one in the TPS design. This is because the treatment boundary under the Euclidean distance one where $X_1 = 0$ and $X_2 = 0$, whereas under the distance measure above, the boundary is one where $X_1 = 0$ or $X_2 = 0$. Consider a unit that nearly misses the cutoff on one dimension but exceeds the cutoff on the other dimension by a large margin. Under the Euclidean distance, this unit would be treated as one that is far from being eligible for treatment, whereas under the distance measure above, this unit would be treated as one that closely misses eligibility. Intuitively, the latter is more in line with the unit's "distance" from eligibility.

The estimand for the rdrobust design is the limit of the average treatment effect as the distance from the treatment boundary approaches zero:

$$\tau = \lim_{d \to 0} \mathbb{E}[Y_i(1) - Y_i(0) \mid d_i = d].$$

This estimand is equivalent to the one for the TPS design. The key to showing this is the mapping from (X_1, X_2) to d_i. The function $T : \mathbb{R}^2 \to \mathbb{R}$ defined Equation 1 for d_i preserves the relative density of observations along the boundary. For small d, the set $\{(X_1, X_2) : T(X_1, X_2) = d\}$ forms a thin band around $\mathcal{B}$. If we denote by $g(d)$ the density of d, then for small d the conditional expectation can be written as

$$\mathbb{E}[Y_i(1) - Y_i(0) \mid d_i = d] = \frac{\int_{T^{-1}(d)} (Y_i(1) - Y_i(0)) f_{\mathbf{X}}(\mathbf{x})\, d\mathbf{x}}{\int_{T^{-1}(d)} f_{\mathbf{X}}(\mathbf{x})\, d\mathbf{x}}.$$

As $d \to 0$, the set $T^{-1}(d)$ converges to $\mathcal{B}$, and hence the limit of the above expression equals the average treatment effect along the boundary,

$$\lim_{d \to 0} \mathbb{E}[Y_i(1) - Y_i(0) \mid d_i = d] = \frac{\int_{\mathcal{B}} \tau_{\mathbf{x}} f_{\mathbf{X}}(\mathbf{x})\, d\mathbf{x}}{\int_{\mathcal{B}} f_{\mathbf{X}}(\mathbf{x})\, d\mathbf{x}}.$$

I evaluate the designs for two scenarios, one with heterogeneity in treatment effects and one without. In both scenarios, I set the treatment effect to around -0.005. For the bootstrap in designs 1-4, I use 10,000 bootstrap samples. I run the simulation 5,000 times for each design.

In each iteration of the simulation, I draw cutoff values (x_1^*, x_2^*) from two independent uniform distributions. For x_1^*, the value is sampled uniformly between the 35th and 65th percentiles of the X_1 distribution, and for x_2^*, the value is sampled uniformly between the 45th and 75th percentiles of the X_2 distribution. This is to keep the average number of treated units in a narrow range from the actual number of treated units in the data. I choose these ranges because they are close to the actual cutoffs in the data: the cutoff for X_1 is around the 55th percentile and that for X_2 the 65th percentile.[13]

For the scenario without treatment effect heterogeneity, I set the treatment effect to be -0.005. For the scenario with treatment effect heterogeneity, the effect size varies across the simulations because it changes with the cutoff value for X_1 and the density of the running variables at the cutoff. I set the treatment effect to be $-0.001 - (X_1)^2/150$, which corresponds to an effect size of around -0.005 on average across the simulations.

To calculate the true treatment effect for each simulation, I first form a grid of points along the treatment boundary. I then use local likelihood regression to estimate the empirical density of the running variables at these grid points and normalize the estimates first along each boundary and then across the two boundaries so that they sum to one both on each

[13] I set the lower bounds to be further away from the actual cutoffs than the upper bounds so that the average number of treated units across the simulations is closer to the actual number of treated units in the data.

boundary and across the two boundaries. Next, I compute the true treatment effect at each point on the grid: $-0.001 - (X_1)^2/150$. These predicted effects are then weighted by the normalized density. Finally, I aggregate the weighted treatment effects across the entire grid to obtain the overall average treatment effect. For each simulation, this is the true treatment effect against which the estimates are compared.

I calculate the power as the proportion of estimates that are statistically significant at the 5% level and the coverage as the proportion of confidence intervals that contain the true treatment effect. For the thin plate spline (TPS) designs, I also calculate the power and coverage at an α level of 0.1.

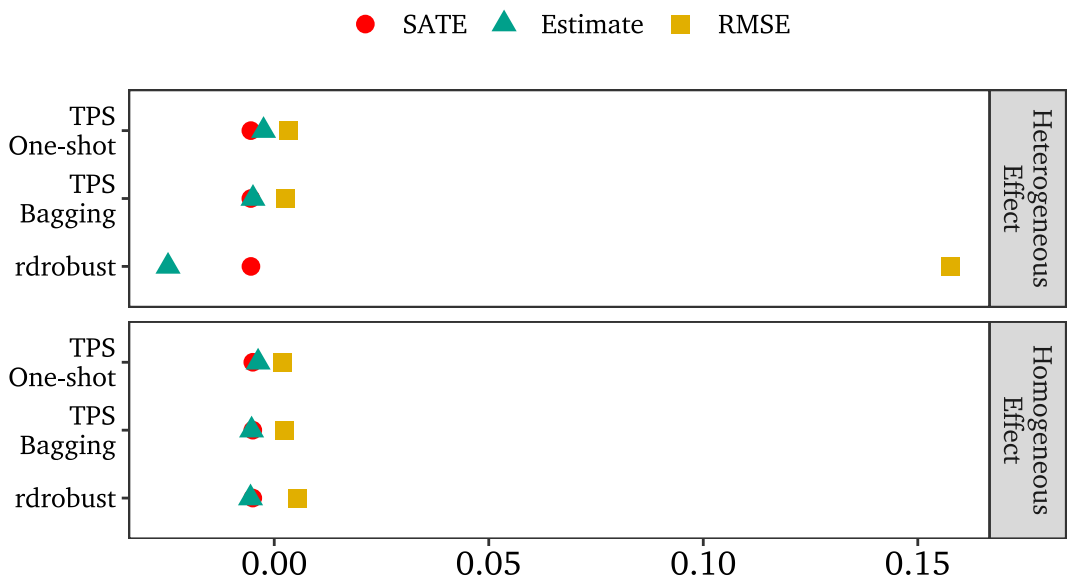

Figure 5: Summary statistics of estimates for the six designs in the simulation study. TPS: thin plate splines; SATE: (true) sample average treatment effect; RMSE: root mean squared error.

Figure 5 shows the mean and root mean squared error (RMSE) of the point estimates for the six designs in the simulation study. TPS with bagging has the least bias and, when treatment effects are heterogeneous, the smallest RMSE. rdrobust is largely unbiased when treatment effects are homogeneous, but the bias becomes substantial (549%) when treatment effects are heterogeneous. The RMSE is the highest for the rdrobust designs in both

scenarios. The results are also available in tabular form in Appendix Table 4.

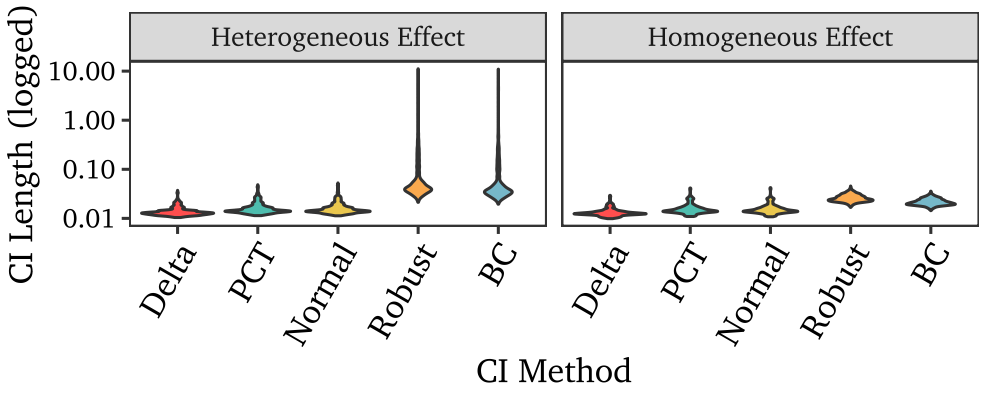

Figure 6: Violin plot of confidence interval (CI) lengths (logged) for the six designs. Delta: delta bootstrap confidence intervals for thin plate splines (TPS) + Bagging; PCT: percentile bootstrap CIs for TPS or TPS + Bagging; Normal: bootstrap with normal approximation for TPS; Robust: robust CIs from rdrobust; Bias-corrected: bias-corrected CIs from rdrobust.

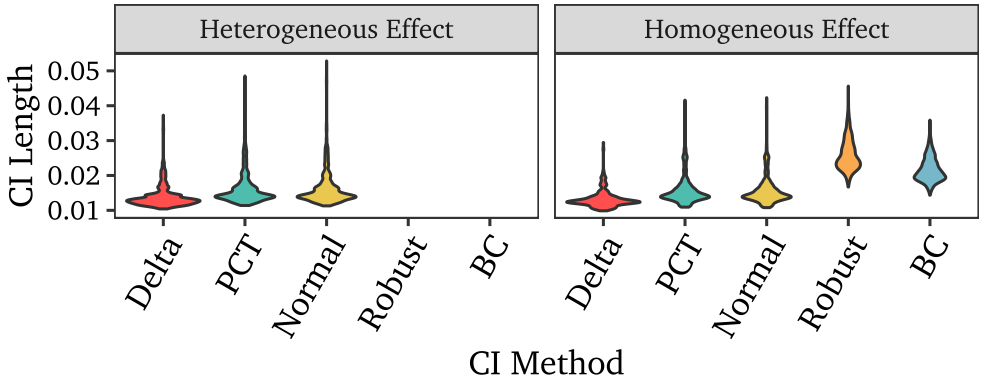

Figure 7: Violin plot of confidence interval (CI) lengths for the bootstrap methods. Delta: delta bootstrap confidence intervals for thin plate splines (TPS) + Bagging; PCT: percentile bootstrap CIs for TPS or TPS + Bagging; Normal: bootstrap with normal approximation for TPS.

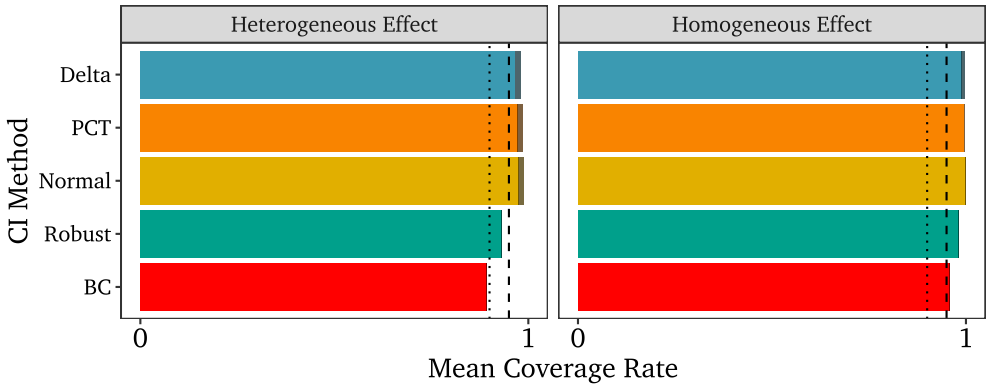

Figure 8: Bar plot of coverage rates for the six designs. TPS: thin plate splines. Delta: delta bootstrap confidence intervals (CIs) for thin plate splines (TPS) + Bagging; PCT: percentile bootstrap CIs for TPS or TPS + Bagging; Normal: bootstrap with normal approximation for TPS; Robust: robust CIs from rdrobust; Bias-corrected: bias-corrected CIs from rdrobust. For Delta, PCT, and Normal, the bars denote the coverage of 90% CIs, and grey-shaded areas denote extra coverage of 95% CIs. For Robust and BC, the bars denote the coverage of 95% CIs. The dashed line denotes 0.95 and the dotted line denotes 0.9.

Figure 6 and Figure 7 show the distributions of confidence interval lengths for the six designs. The lengths are log-10 transformed in Figure 6 because the lengths from the two rdrobust CIs are highly skewed when treatment effect are heterogeneous. The bootstrap CIs are also more skewed compared to the case where treatment effects are homogeneous, but the tails are much shorter than the tails of the rdrobust CIs. In both the heterogeneous and homogeneous effect scenarios, the length of delta bootstrap CIs with bagging are shorter on average than the other designs and also more concentrated around the median. The percentile and the normal bootstrap CIs have similar distributions of lengths. They also outperform the rdrobust CIs in terms of length in both scenarios, although the BC CIs have shorter tails than the percentile and normal bootstrap CIs when treatment effects are homogeneous.

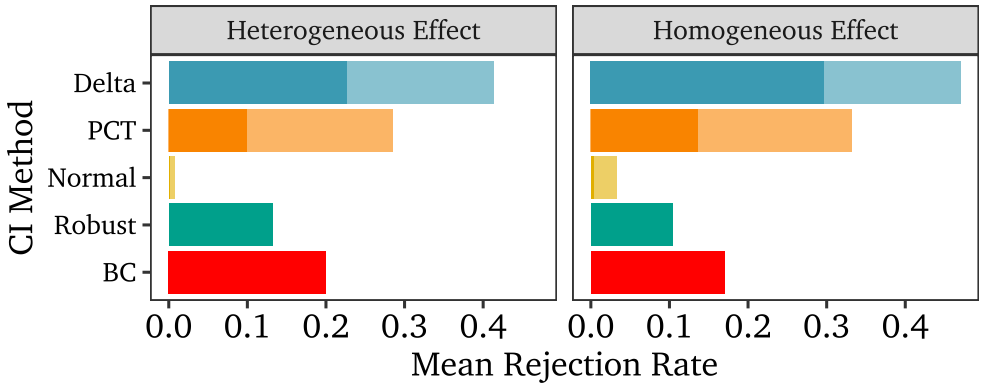

Figure 9: Bar plot of rejection rates for the six designs. Delta: delta bootstrap CIs for TPS + Bagging; PCT: percentile bootstrap CIs for TPS or TPS + Bagging; Normal: bootstrap with normal approximation for TPS; Robust: robust CIs from rdrobust; Bias-corrected: bias-corrected CIs from rdrobust. For Delta, PCT, and Normal, the bars denote the rejection rate of 95% CIs, and darker shaded areas denote the rejection rate of 90% CIs. For Robust and BC, the bars denote the rejection rate of 95% CIs.

Turning to coverage rates (Figure 8), the three bootstrap methods all have highly conservative coverage rates in both scenarios (even the 90% CIs have coverage rates above 95%). The rdrobust CIs have coverage rates close to the nominal level when treatment effects are homogeneous, but they undercover when treatment effects are heterogeneous. The robust CIs undercover slightly, while the BC CIs have coverage rates that are substantially below the nominal level (around 90% for 95% CIs).

The conservativeness of the bootstrap CIs may raise concerns about the power of these tests. However, as Figure 9 shows, among CIs that have close to nominal or conservative coverage rates, the delta bootstrap CIs with bagging have substantially higher rejection rates than the other designs in both scenarios whether using the 90% or 95% CIs. If we use the 95% CIs for rejection decisions, the power is 0.2258 when treatment effects are heterogeneous and 0.296760711 when treatment effects are homogeneous. The 95% bias-corrected CIs from rdrobust has a rejection rate of around 0.2 when treatment effects are heterogeneous, but its coverage is below the nominal level (Figure 8). Moreover, for the rdrobust CIs, conditional on rejection, the proportion of estimates that have the wrong sign using the 95% CIs is around 0.2 when treatment effects are heterogeneous and around 0.03

when effects are homogeneous (Figure 10). The rate of wrong sign estimates is 0 for the TPS designs.

A.4 Deviations from the Pre-analysis Plan (PAP)

1. For covariate adjustment, the PAP stated that I would use a leave-one-out procedure to obtain the predicted vote share for each of the N units (effectively training N models). However, I found that this procedure would lead to bias in the estimation procedure, because the residualized outcomes would no longer be independent. This is because a unit's residualized outcome is obtained via a model that is trained on the rest of the data. This introduces dependence between the residuals, which complicates the estimation of the standard errors. Additionally, because the residuals are used to fit the thin plate splines (TPS), a nonparametric model, the TPS's regularization no longer prevents overfitting as it does when the observations are independent. In the analysis, I use a semi-independent data source that includes only treated counties to train the model and predict the outcome for each county. This data set is not used in the fitting of the TPS models. If there are systematic differences in outcomes between treated and untreated counties in the vicinity of the treatment boundary, this procedure would preserve those differences in the predicted outcomes without introducing overfitting.
2. The PAP stated that I would analyze the data at the county level for the RDD and cluster the standard errors at the SA level. I later realized this procedure would lead to a misalignment between the estimation of the density of the running variables (which is defined at the SA level because the running variables are measured at the SA level) and the estimation of the treatment effect (which is defined at the county level). In the analysis, I estimate the RDD at the SA level instead. Nevertheless, I report the results obtained from a county-level analysis in Section A.5.3 of the Appendix. They are qualitatively similar to the SA-level results.

3. The PAP stated that, in obtaining the estimate of the ATE, I would aggregate the predicted outcomes using the empirical distribution of the running variables and forcing one of the running variable to be at the cutoff value. However, I found that this procedure would lead to substantial bias in the estimation of the treatment effect as it weights values far from the cutoff equally with those close to the cutoff. To address this, I use kernel density estimates of the running variables to weight the predicted outcomes, as described in the main text. This procedure gives more weight to observations near the cutoffs, where the treatment effect is close to being identified.

Table 4: Summary statistics of estimates for the six designs in the simulation study

Method	Heterogeneity	SATE	Estimate	RMSE
TPS Bagging	Heterogeneous Effect	-0.00545	-0.00496	0.00267
TPS One-shot	Heterogeneous Effect	-0.00545	-0.00249	0.00336
rdrobust	Heterogeneous Effect	-0.00544	-0.02480	0.15800
TPS Bagging	Homogeneous Effect	-0.00500	-0.00528	0.00234
TPS One-shot	Homogeneous Effect	-0.00500	-0.00377	0.00181
rdrobust	Homogeneous Effect	-0.00500	-0.00553	0.00544

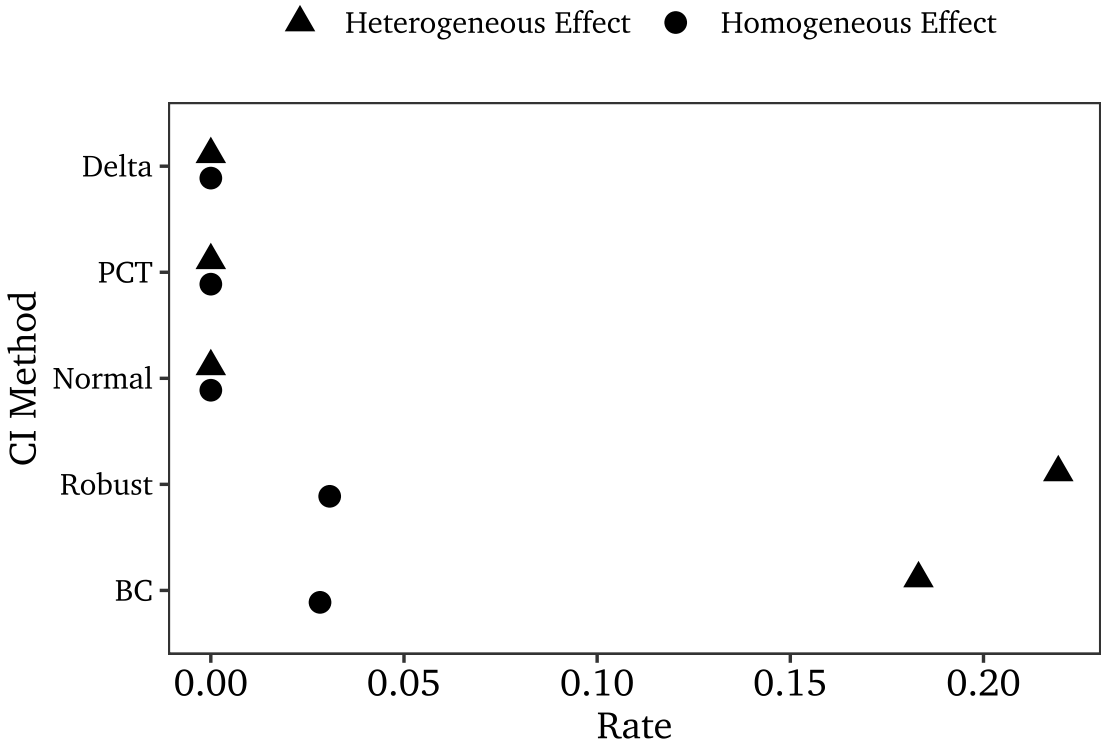

Figure 10: Mean rate of point estimate having the wrong sign conditional on rejection. Delta: delta bootstrap confidence intervals (CIs) for thin plate splines (TPS) + Bagging; PCT: percentile bootstrap CIs for TPS or TPS + Bagging; Normal: bootstrap with normal approximation for TPS; Robust: robust CIs from rdrobust; BC: bias-corrected CIs from rdrobust.

A.5 Additional Results and Figures

A.5.1 Percentile Bootstrap Estimates

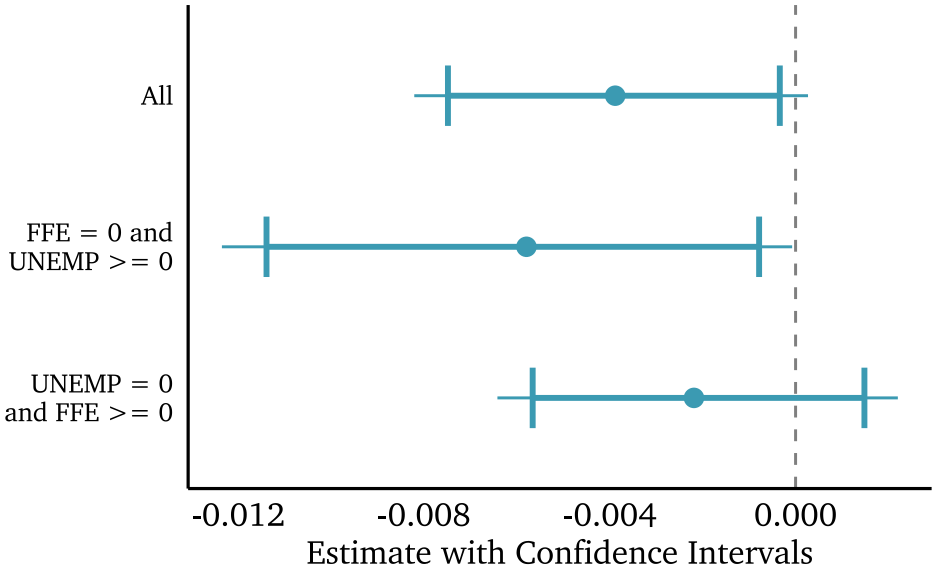

Figure 11: Point estimates for both boundaries combined and each individually with 95% and 90% percentile confidence intervals (CIs). N = 403. The narrower ranges bounded by bars are 90% CIs and the wider ones are 95% CIs.

The 95% confidence interval from the percentile bootstrap is $(-0.0082, 0.0003)$ (Figure 11), and the p-value is 0.070. As simulation results in Section A.3 suggest, the percentile bootstrap has conservative coverage, so the confidence interval from the percentile bootstrap is likely too wide. While the delta bootstrap confidence interval is also conservative, it is narrower and has a coverage rate closer to the nominal level.

A.5.2 Excluding SAs with No Fossil Fuel Employment

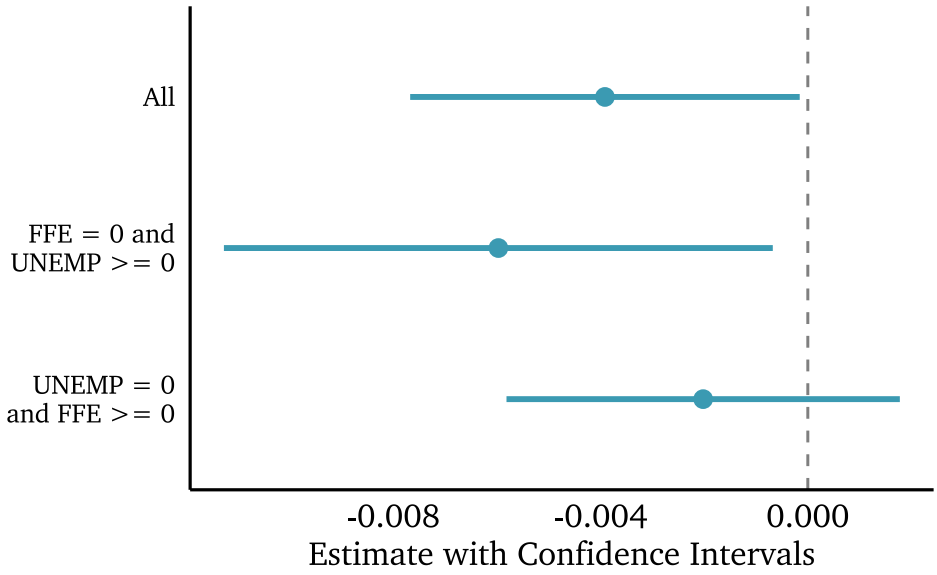

Figure 12: Point estimates for both boundaries combined and each individually with 95% delta confidence intervals (CIs). Data excludes SAs with no fossil fuel employment. N = 393.

Figure 12 shows the point estimates when SAs with no fossil fuel employment are excluded from the analysis. The point estimate is -0.00392, the 95% confidence interval from the delta bootstrap is $(-0.00768, -0.000156)$, and the p-value is 0.0412. The results are similar to those in the main analysis, suggesting that the inclusion of SAs with no fossil fuel employment does not substantially affect the results.[14]

[14]The data truncation procedure in the PAP would keep SAs with no fossil fuel employment in the analysis sample.

A.5.3 County-level Analysis

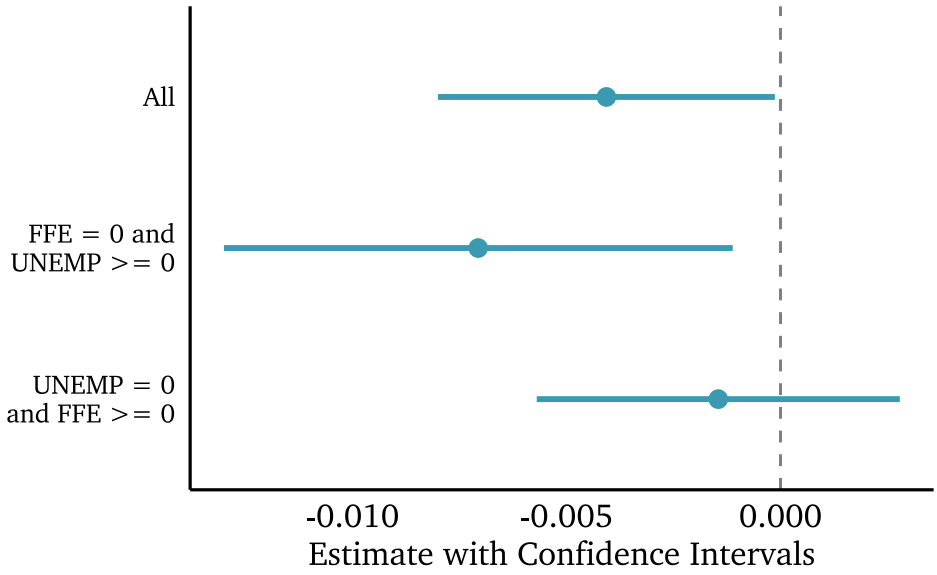

Figure 13: Point estimates for both boundaries combined and each individually with 95% delta confidence intervals (CIs). Analysis is at the county level with confidence intervals clustered at the SA level. N = 2168. Confidence intervals are obtained from a delta cluster-bootstrap with 10,000 replications.

Figure 13 shows the point estimates when the analysis is conducted at the county level. The point estimate is -0.00407, the 95% confidence interval from the delta cluster-bootstrap is $(-0.00800, -0.000131)$, and the p-value is 0.0429. The results are qualitatively similar to those in the SA-level analysis.

A.5.4 One-shot Predictions

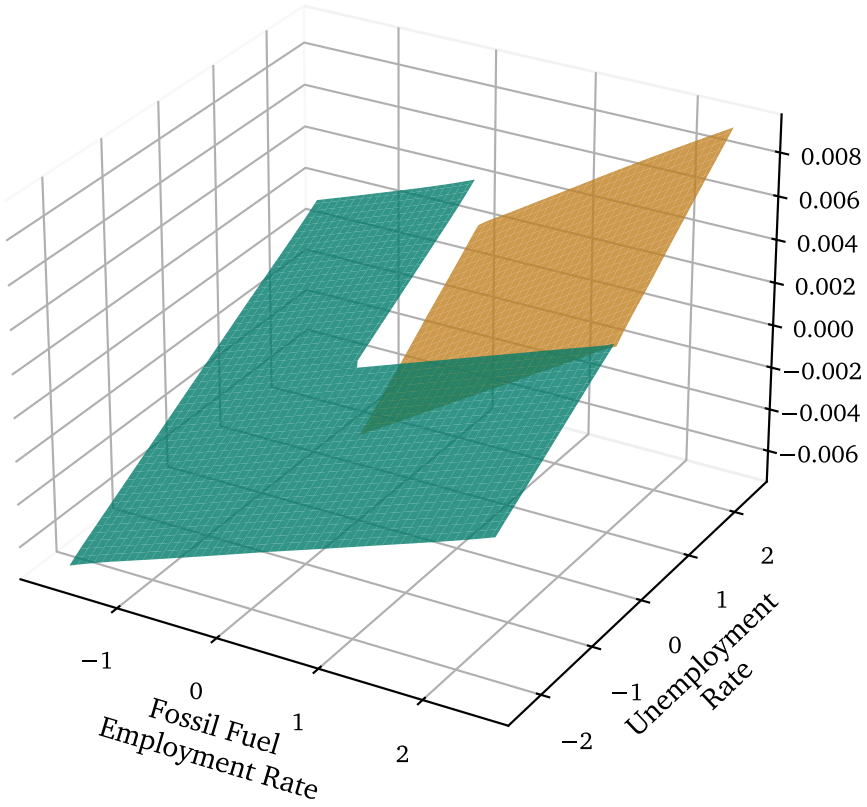

Figure 14: Fitted surfaces for the residualized Democratic vote share in SA-level Energy Communities vs. other SAs in the 2024 presidential election. The larger surface on the left is the untreated region. Predictions are from a one-shot undersmoothed thin plate spline model.

Figure 14 shows the fitted surfaces for the residualized Democratic vote share in the 2024 presidential election. Predictions are from a one-shot undersmoothed thin plate spline model. The surfaces are substantially smoother than those in Figure 4. This is because the predictions are based on a single model fit to the data; i.e., the predictions are obtained from an insample fit.